Journal of Oral Biology and Craniofacial Research 16 (2026) 101424

Contents lists available at ScienceDirect

Journal of Oral Biology and Craniofacial Research

journal homepage: www.elsevier.com/locate/jobcr

Ovine bone graft enhances osteogenic commitment in human osteoblasts via selective suppression of miR-6797-5p: In silico and in vitro study

Aparna Sethi [a,f], Khushali K Shah [a,f], Dhanraj Ganapathy [a], Shahabe Saquib Abullais [b,c], Abdulmajeed Almuaddi [d], Saravanan Sekaran [e,*]

[a] Department of Prosthodontics, Saveetha Dental College and Hospitals, Saveetha Institute of Medical and Technical Sciences, Saveetha University, Chennai, 600077, Tamil Nadu, India
[b] Department of Periodontics and Community Dental Science, King Khalid University, College of Dentistry, Abha, 61421, Saudi Arabia
[c] Department of Periodontology, Faculty of Dental Medicine, Universitas Airlangga, Indonesia
[d] Division of Periodontics, Department of Periodontics and Community Dental Sciences, College of Dentistry, King Khalid University, Abha, Saudi Arabia
[e] Saveetha Institute of Basic Medical Sciences (SIBMS), Saveetha Institute of Medical and Technical Sciences, Saveetha University, Chennai, 602105, Tamil Nadu, India

ARTICLE INFO

Keywords:
Ovine bone graft
Hydroxyapatite
RUNX2
microRNA
Osteogenesis
Conditioned medium
Biomaterials

ABSTRACT

Background: Xenogeneic grafts are widely employed in oral and maxillofacial rehabilitation, but their biological influence extends beyond osteoconduction. Central to osteoblast differentiation is the transcription factor RUNX2, which is tightly regulated by networks of microRNAs (miRNAs). While the osteogenic effects of bovine and porcine grafts have been well studied, little is known about whether ovine bone grafts can alter RUNX2-related post-transcriptional regulation. This study aimed to investigate whether ovine bone graft–derived soluble factors modulate RUNX2-associated miRNAs and thereby influence osteogenic commitment in human osteoblast-lineage cells.

Methods: Hydroxyapatite was isolated from ovine femoral bone and used to prepare conditioned medium (OBG-CM). Human osteoblastic cells and mesenchymal stem cells were exposed to OBG-CM for 24 h. Candidate RUNX2-targeting miRNAs were first identified in silico using miRDB and STarMir, with overlapping predictions screened by qRT-PCR. Predicted binding was further analysed by TargetScan. Functional assays were carried out by transfecting cells with hsa-miR-6797-5p mimics and inhibitors, followed by assessment of RUNX2 mRNA and protein expression.

Results: Computational analysis highlighted several high-confidence RUNX2-targeting miRNAs, including hsa-miR-6797-5p. Exposure to OBG-CM selectively reduced the expression of hsa-miR-6797-5p, hsa-miR-889-5p and hsa-miR-122-5p, while other candidates showed minimal change. TargetScan identified a conserved 8-mer seed match for hsa-miR-6797-5p within the RUNX2 3′UTR. Transfection with the mimic suppressed RUNX2 expression at both transcript and protein levels, whereas inhibition produced the opposite effect.

Conclusions: Ovine bone graft–derived factors can selectively remodel the miRNA landscape in osteoblast-lineage cells. These insights may guide the development of bioactive grafts optimised for post-transcriptional regulation.

1. Introduction

Bone augmentation is integral to contemporary oral and maxillofacial rehabilitation, yet the field still balances biological efficacy, safety, and patient acceptability when choosing graft materials.[1] Autogenous bone remains the performance benchmark but is constrained by donor-site morbidity and limited volumes; hence clinicians frequently employ allografts, xenografts, and synthetics as osteoconductive scaffolds or as carriers for pro-osteogenic cues.[2] Beyond material science, patient values and cultural considerations influence graft selection; multicenter surveys and ethical analyses show that concerns about animal use and disease transmission shape acceptance of xenografts, underscoring the need for transparent, preference-sensitive decision-making.[3] While bovine and porcine xenografts dominate dental practice,

* Corresponding author.
E-mail addresses: aparnasethidental@gmail.com (A. Sethi), khushali.shah30@gmail.com, khushalik.sdc@saveetha.com (K.K. Shah), drnallu@gmail.com (D. Ganapathy), saravanans.sdc@saveetha.com (S. Sekaran).
[f] Equally contributed.

https://doi.org/10.1016/j.jobcr.2026.101424
Received 29 September 2025; Received in revised form 3 January 2026; Accepted 11 February 2026
Available online 20 February 2026

interest in ovine-derived bone mineral has grown for two practical reasons: (i) the physicochemical tunability of sheep-bone-derived hydroxyapatite (HA), and (ii) the long-standing use of sheep as a translational large-animal model for bone healing, whose mineral composition and remodeling dynamics approximate those of humans. Recent in-vitro reports show that HA generated from ovine bone can be surface-modified (e.g., with L-leucine or L-arginine) to refine crystallinity, pore architecture, and osteogenic cell behavior, and has been benchmarked against widely used xenografts such as Bio-Oss. Clinical translation remains early, but these data motivate mechanistic inquiry.[4,5] Natural bone–derived hydroxyapatite (HA) has attracted considerable attention in recent years due to its close compositional and structural similarity to human bone mineral. Among animal sources, camel bone has emerged as a promising and underexplored precursor for biologically derived HA. Camel skeletal tissue is characterized by a dense cortical architecture and a mineral phase enriched with calcium and phosphate ions in ratios closely approximating stoichiometric hydroxyapatite, making it particularly suitable for biomedical applications. Several studies have demonstrated that hydroxyapatite isolated from camel bone exhibits high crystallinity, thermal stability, and favorable Ca/P ratios following controlled thermal or chemical processing. Compared with synthetic HA, camel bone–derived HA retains trace ionic substitutions (such as Mg^{2+}, Na^{+}, and carbonate groups) that naturally occur in biological apatite and are known to enhance osteoblast adhesion, proliferation, and differentiation. These intrinsic substitutions contribute to improved bioactivity and more physiologically relevant interactions with bone-forming cells [6–8].

Parallel literature in preclinical orthopedics documents why sheep biology is appealing for scaffold testing—sheep bone micro/macrostructure and remodeling rates are broadly comparable to humans, making ovine tissues and models informative for biomaterial–bone crosstalk.[9,10] Osteoblasts arise from mesenchymal precursors through a staged program—commitment, matrix production, and mineralization—controlled by converging signalling axes (canonical/non-canonical Wnt, BMP/TGF-β, Hedgehog, Notch, FGF/IGF, Hippo) and by mechanotransducive inputs (e.g., Piezo1/2). This network interfaces with epigenetic regulators to coordinate expression of lineage markers (ALPL, COL1A1, SP7/OSX, IBSP, BGLAP/OCN). Authoritative syntheses published in 2024 emphasize that pathway cross-talk is the rule rather than the exception, and that transcriptional "master switches" operate within this signal-rich context.[11]

RUNX2 is indispensable for commitment to the osteoblast lineage and for timely progression through early differentiation. It collaborates with CBFβ and SP7/OSX to activate bone matrix genes, and it integrates BMP and Wnt inputs to maintain osteogenic identity.[12] Newer functional genomics show that RUNX2 does more than transactivate; it can establish chromatin accessibility at osteoblast-specific enhancers, behaving as a pioneer-like factor that shapes lineage-defining regulatory landscapes in vivo. Together, these insights explain why modest changes in RUNX2 dosage, stability, or cofactor availability can have outsized effects on bone formation.[13] MicroRNAs (miRNAs) are known to regualte several human diseases and pahysiological processes [14–16]. They add a post-transcriptional layer that fine-tunes osteogenic signaling and transcriptional output. Classic and contemporary studies converge on a RUNX2-centered miRNA network: miR-204/211 directly repress RUNX2 and tilt MSC fate away from osteogenesis; the miR-30 family dampens BMP-2–driven differentiation by targeting RUNX2 (and SMAD1); other RUNX2-targeting miRNAs include miR-133/135, miR-34c, miR-23a/27a/24-2 (which also intersect with SATB2), forming feedback circuits that balance matrix gene expression and maturation. Conversely, pro-osteogenic miRNAs (e.g., miR-26a, miR-29 family, miR-181 clusters) and exosomal miRNA cargo can enhance osteoblast activity and bone formation in vitro and in vivo.[17,18] Importantly for biomaterials research, scaffolds and nanoparticles can deliver or modulate miRNAs locally—HA-based carriers have been used to raise intracellular levels of osteogenic miRNAs and augment mineralization; miRNA-activated scaffolds (e.g., miR-26a) have improved bone repair quality in animal models.[19,20] Up-to-date reviews chart this miRNA landscape across bone formation, remodeling, and extracellular-vesicle biology, highlighting translational opportunities.[21,22]

Given (i) the emerging evidence that ovine-derived HA scaffolds present distinct surface chemistry and microarchitecture, and (ii) the centrality of miRNA networks in calibrating RUNX2 activity and osteogenic signalling, a logical next question is whether exposure to an ovine xenograft shifts the miRNA repertoire of osteoblast-lineage cells in ways that favour or hinder differentiation. Defining such graft-mediated miRNA signatures—particularly those converging on RUNX2 and BMP/Wnt nodes—offers a mechanistic bridge between surface/material properties and cellular fate decisions, and could inform rational graft optimization. Accordingly, the present study was designed to identify early post-transcriptional regulatory responses to ovine bone graft–derived soluble factors, rather than to directly assess terminal osteogenic differentiation.

2. Materials and methods

2.1. In silico analyses on RUNX2 and miRNA interaction

The 3′ untranslated region (UTR) sequence of RUNX2 was retrieved from the Ensembl BioMart database. The updated list of all human microRNA (miRNA) sequences was obtained from the miRBase database. To predict potential miRNAs targeting RUNX2, two parallel in silico approaches were used. In the first, the miRNA name was directly queried in miRDB, while in the second, the retrieved 3′UTR sequence of RUNX2 was input into STarMir for structural interaction predictions. Both datasets were then compared using Venny 2.1.0 to identify overlapping candidate miRNAs predicted by both tools. From this list, experimentally validated miRNAs were eliminated using TarBase and manual PubMed searches, resulting in a refined subset of unvalidated miRNAs, including hsa-miR-5703, with LogitProb scores >0.8. This score threshold ensured the selection of candidates with high predicted binding confidence.

2.2. Preparation of bone graft and isolation of hydroxyapatite

Bone is composed of organic (proteins, lipids) and inorganic (hydroxyapatite, calcium carbonate, oxides, and phosphates) fractions. To isolate the inorganic hydroxyapatite (HA), it is necessary to eliminate the organic components first. For this study, mid-diaphyseal segments of ovine femur were collected and cut into sizeable slices after carefully removing any adhering soft tissue. To extract marrow and intrinsic fluids, the bone sections were boiled at 100 °C for 12 h. Following this, the samples were cooled and stored at 4 °C for 12 h, then oven-dried at 100 °C for another 12 h to ensure complete dehydration. Any remaining soft tissue was manually removed before proceeding with chemical treatment. Organic remnants such as lipids and proteins were further extracted using a thermal-assisted process, followed by immersion in ethanol for 12 h to remove residual solvents. The samples were then subjected to a second oven-drying step at 100 °C for 12 h. To enhance removal of stubborn organic residues, the specimens were treated with 150 mL of ethylenediamine (Sisco Research Laboratories Pvt. Ltd., Mumbai, India; Cat. No. 70790) for 48 h, using an HME 250 unit (Labquest, Mumbai, India). After treatment, dual ethanol washes were performed to ensure complete clearance of the reagent. Finally, the deproteinised bone specimens were subjected to sintering at 320 °C for 3 h in a muffle furnace (Aadarsh Technologies, Mumbai, India), resulting in purified hydroxyapatite suitable for further experimental use.

2.3. Cell culture

Human osteoblastic cells were obtained from a NCCS, Pune, India and maintained under standard culture conditions. Cells were grown in

Dulbecco's Modified Eagle Medium (DMEM) supplemented with 10% fetal bovine serum (FBS), 1% penicillin-streptomycin, and incubated at 37 °C in a humidified atmosphere containing 5% CO_2. Cells were subcultured upon reaching 70–80% confluency and used between passages 3–6 for all experiments.

2.4. Ovine Bone Graft-Conditioned Medium (OBG-CM)

Conditioned medium was prepared by incubating sterile ovine bone graft material (obtained under ethical approval (SRB/SDC/PROSTHO-2105/22/011) and processed in-house based on our pervious study[23]) in serum-free DMEM at a concentration of 100 mg/mL for 48 h at 37 °C. The supernatant was collected, centrifuged at 3000 rpm for 10 min, and filtered through a 0.22 μm membrane filter to remove particulate matter. Human osteoblastic cells were seeded in 6-well plates at a density of 2×10^5 cells/well and allowed to attach for 24 h. Subsequently, the culture medium was replaced with 100% OBG-conditioned medium (OBG-CM) and incubated for 24 h. Control groups were maintained in parallel using standard culture medium.

2.5. Realtime PCR analysis

After 24 h of exposure, total RNA including miRNA was extracted from cells using the miRNeasy Mini Kit (Qiagen) following the manufacturer's instructions. RNA purity and concentration were assessed using a NanoDrop spectrophotometer. For miRNA-specific expression, cDNA synthesis was performed using the TaqMan™ Advanced miRNA cDNA Synthesis Kit (Applied Biosystems). Expression levels of hsa-miR-5703 and other selected RUNX2-targeting miRNAs were quantified by qRT-PCR using SYBR Green chemistry and specific primers. U6 small nuclear RNA was used as the endogenous control. The ΔΔCt method was used to calculate relative fold changes in expression compared to untreated controls. Total RNA was reverse-transcribed using High-Capacity cDNA Reverse Transcription Kit (Applied Biosystems). RUNX2 mRNA levels were quantified by qPCR using gene-specific primers, with GAPDH as the internal reference. All reactions were performed in triplicates, and the fold change in gene expression was determined using the ΔΔCt method.

2.6. Western blotting for RUNX2 protein expression

Total protein was extracted using RIPA buffer containing protease and phosphatase inhibitors. Protein concentration was quantified using the BCA protein assay kit (Pierce). Equal amounts of protein (30 μg) were resolved on 10% SDS-PAGE gels and transferred to PVDF membranes. After blocking with 5% non-fat dry milk in TBST, membranes were incubated overnight at 4 °C with primary antibodies against RUNX2 (1:1000) and β-actin (1:2000) as the loading control. Blots were probed with HRP-conjugated secondary antibodies and visualized using enhanced chemiluminescence (ECL).

2.7. Functional validation of hsa-miR-6797-5p targeting RUNX2

To confirm the regulatory role of hsa-miR-6797-5p on RUNX2 expression, human osteoblastic cells were transfected with either miR-6797-5p mimic or inhibitor, along with respective negative controls, using Lipofectamine RNAiMAX (Thermo Fisher). Post-transfection (24h), RNA and protein were isolated for qRT-PCR and Western blot analysis of RUNX2 expression.

2.8. Statistical analysis

All assays were carried out with three independent biological replicates, and the full set of experiments was reproduced in at least three separate runs, unless indicated otherwise. Results are reported as mean ± SD. Statistical comparisons between two groups were conducted using an unpaired two-tailed Student's t-test.

3. Results

3.1. Identification of RUNX2-targeting miRNAs by in silico prediction

Computational screening was performed to identify miRNAs with potential binding sites within the 3′UTR of RUNX2. Predictions generated independently by the miRDB and STarMir platforms were compared. The Venn analysis (Fig. 1) showed that a total of 263 candidate miRNAs were predicted across both databases. Of these, 136 miRNAs (51.7%) were consistently identified by both tools, highlighting a robust subset of overlapping candidates. In contrast, 127 miRNAs (48.3%) were uniquely predicted by miRDB, whereas no exclusive candidates emerged from STarMir. To refine this list, candidate miRNAs were prioritized according to the Logit Probability (LogitProb) scores provided by miRDB. The top 15 miRNAs with LogitProb >0.8 are displayed in Fig. 1. Notably, hsa-miR-4455 ranked highest with a LogitProb score of 0.911, followed by hsa-miR-5703 (0.888) and several others including hsa-miR-4434, hsa-miR-4516, and hsa-miR-4659a/b-5p, each scoring 0.873. These values indicate strong binding probabilities between the selected miRNAs and the RUNX2 3′UTR. From the high-confidence set, experimentally validated miRNAs were excluded using TarBase and literature screening. This process yielded a refined group of novel, unvalidated candidates, including hsa-miR-5703, which was carried forward for downstream functional studies. Additionally, hsa-miR-6797-5p, identified within the high-confidence group, was shortlisted for independent validation of its regulatory potential on RUNX2 expression.

3.2. Expression of candidate miRNAs in osteoblasts exposed to ovine bone graft–conditioned medium

To determine whether soluble factors released from the ovine xenograft influence RUNX2-targeting miRNAs, human osteoblastic cells were cultured in ovine bone graft–conditioned medium (OBG-CM) for 24 h. Total RNA was then extracted, and the expression of selected high-confidence miRNAs (hsa-miR-4455, hsa-miR-5703, hsa-miR-4434, hsa-miR-4516, hsa-miR-4659a-5p, hsa-miR-4659b-5p, and hsa-miR-5590-5p) was quantified by qRT-PCR. As shown in Fig. 2, the relative fold changes of these miRNAs in OBG-CM–treated cells were comparable to those observed in untreated controls, with mean values clustering around unity. Minor variations were observed across individual candidates—for example, hsa-miR-5703 and hsa-miR-4659a-5p showed a modest upward trend, while hsa-miR-4516 appeared slightly reduced—but none of these differences reached statistical significance within the tested conditions.

These findings suggest that exposure to ovine bone graft–derived soluble cues does not markedly perturb the expression of the tested RUNX2-targeting miRNAs within 24 h, though subtle shifts may indicate the onset of early regulatory changes. Further studies with extended incubation times, dose-response assays, and functional perturbation experiments will be required to clarify whether these small changes contribute meaningfully to RUNX2 regulation and osteoblast differentiation.

3.3. Differential modulation of RUNX2-targeting miRNAs by ovine bone graft–conditioned medium

To further explore the regulatory effects of ovine xenograft-derived soluble factors, an additional panel of high-confidence RUNX2-targeting miRNAs was assessed in osteoblasts following 24-h exposure to OBG-CM. As shown in Fig. 3, most of the tested candidates—including hsa-miR-4776-3p, hsa-miR-890, hsa-miR-5004-3p, and hsa-miR-4423-3p—displayed expression patterns that were broadly similar to untreated controls, with only minor fluctuations.

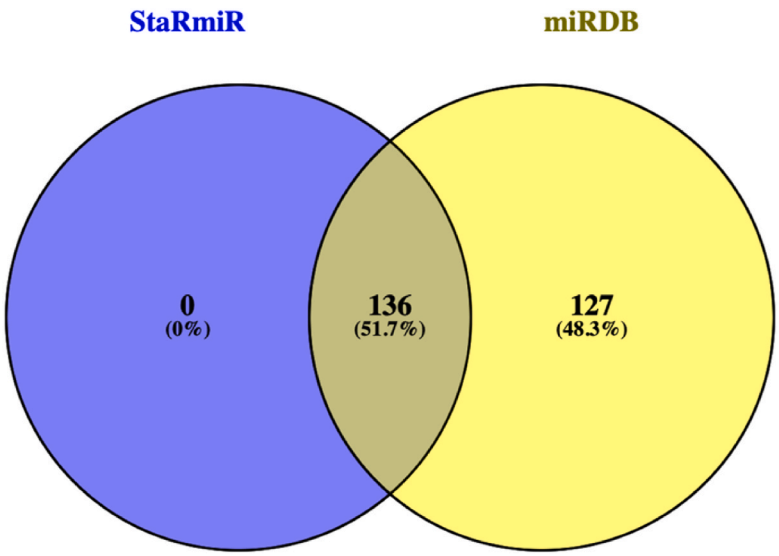

miRNA	LogitProb†
hsa-miR-4455	0.911
hsa-miR-5703	0.888
hsa-miR-4434	0.873
hsa-miR-4516	0.873
hsa-miR-4659a-5p	0.873
hsa-miR-4659b-5p	0.873
hsa-miR-5590-5p	0.873
hsa-miR-122-5p	0.871
hsa-miR-4776-3p	0.866
hsa-miR-890	0.855
hsa-miR-5004-3p	0.842
hsa-miR-6797-5p	0.836
hsa-miR-889-5p	0.823
hsa-miR-4423-3p	0.818
hsa-miR-4651	0.818

Fig. 1. Comparison of predicted miRNAs targeting Runx2 gene from two databases (StaRmiR and miRDB) and top-ranked miRNAs based on Logit Probability scores. The Venn diagram illustrates the overlap between miRNAs predicted to target Runx2 by StaRmiR (blue) and miRDB (yellow). A total of 136 miRNAs (51.7%) were commonly identified by both databases, while 127 miRNAs (48.3%) were uniquely predicted by miRDB. Notably, StaRmiR did not yield any exclusive miRNA predictions in this dataset. On the right, a table displays the top 15 miRNAs targeting Runx2, ranked by their Logit Probability (LogitProb†) scores derived from miRDB. These scores reflect the confidence level of each miRNA-mRNA interaction prediction, with higher values indicating stronger predicted interactions. (For interpretation of the references to colour in this figure legend, the reader is referred to the Web version of this article.)

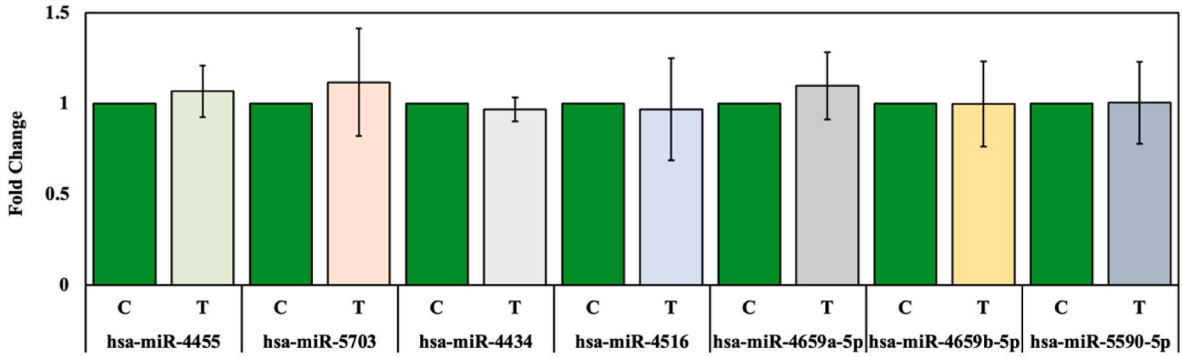

Fig. 2. Expression profile of top candidate miRNAs targeting Runx2 in human osteoblastic cells upon treatment with ovine bone graft-conditioned medium. Human osteoblastic cells were incubated with 100% conditioned medium (CM) derived from ovine bone graft (OBG)for 24 h. Following treatment, total RNA was isolated and real-time RT-PCR was performed to assess the expression levels of selected miRNAs predicted to target Runx2. The graph shows the relative expression levels (mean ± SD) of individual miRNAs normalized to endogenous control (e.g., U6). Colored bars denote different miRNAs corresponding to high-confidence predictions based on prior in silico screening. The analysis highlights subtle changes in expression levels among the candidate miRNAs, suggesting potential regulatory effects of OBG-derived soluble factors on Runx2-associated miRNA networks in osteoblasts. Further validation is required to determine the functional significance of these changes.

In contrast, three miRNAs exhibited clear downregulation in response to OBG-CM. hsa-miR-122-5p showed a statistically significant reduction compared with controls, while hsa-miR-6797-5p and hsa-miR-889-5p demonstrated more pronounced suppression, reaching less than half of control levels. Since all three are predicted repressors of RUNX2, their downregulation suggests a potential derepression of RUNX2 expression, thereby favoring osteogenic gene activation. Taken together, these findings indicate that ovine bone graft–derived factors may exert selective effects on the miRNA landscape of osteoblasts rather than eliciting a uniform global response. By downregulating a subset of inhibitory miRNAs, OBG-CM may contribute to a regulatory environment that supports osteogenic differentiation. However, further functional assays are required to confirm whether these miRNA shifts translate into measurable increases in RUNX2 mRNA and protein expression.

3.4. Validation of hsa-miR-6797-5p as a regulator of RUNX2

To further substantiate the role of specific miRNAs in regulating RUNX2, a subset of candidates was evaluated in mesenchymal stem cells (MSCs) treated with ovine bone graft–conditioned medium (OBG-CM). As shown in Fig. 4a, the expression of hsa-miR-6797-5p was significantly reduced compared to untreated controls, while hsa-miR-122-5p and hsa-miR-889-5p remained largely unchanged. This selective downregulation highlights hsa-miR-6797-5p as a responsive candidate miRNA influenced by xenograft-derived soluble factors. To probe the mechanistic basis of this regulation, in silico target analysis was performed using TargetScan, which predicted a strong binding site for hsa-miR-6797-5p within the 3′ untranslated region (UTR) of RUNX2 mRNA. As shown in Fig. 4b, the predicted duplex displayed a perfect 8-mer seed pairing between the miRNA and RUNX2 3′UTR (positions 2591–2598), indicative of a high-confidence and specific interaction. Together, these results suggest that hsa-miR-6797-5p may act as a direct post-transcriptional

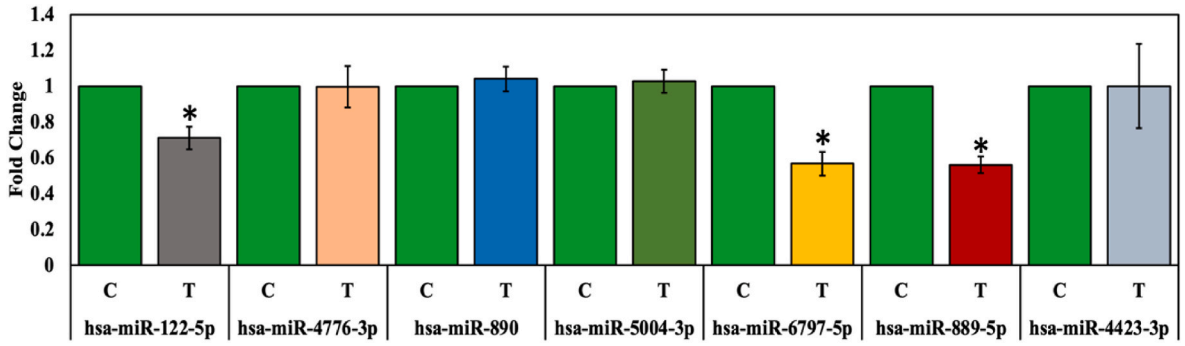

Fig. 3. Expression of Runx2-targeting miRNAs in human osteoblastic cells treated with ovine bone graft-conditioned medium. Human osteoblastic cells were treated with 100% conditioned medium (CM) obtained from ovine bone graft (OBG)for 24 h. Post-treatment, total RNA was extracted and the expression of selected miRNAs targeting Runx2 was quantified using real-time RT-PCR. The bar graph shows the relative expression levels (mean ± SD) of individual miRNAs, normalized to a housekeeping small RNA (U6). Distinct downregulation was observed in hsa-miR-889-5p and hsa-miR-890, suggesting potential derepression of Runx2. Other miRNAs remained relatively unchanged or showed minor fluctuations. These findings imply that OBG-derived factors may modulate osteogenic differentiation by selectively altering the miRNA landscape in osteoblasts. Further studies are needed to validate these regulatory effects functionally.

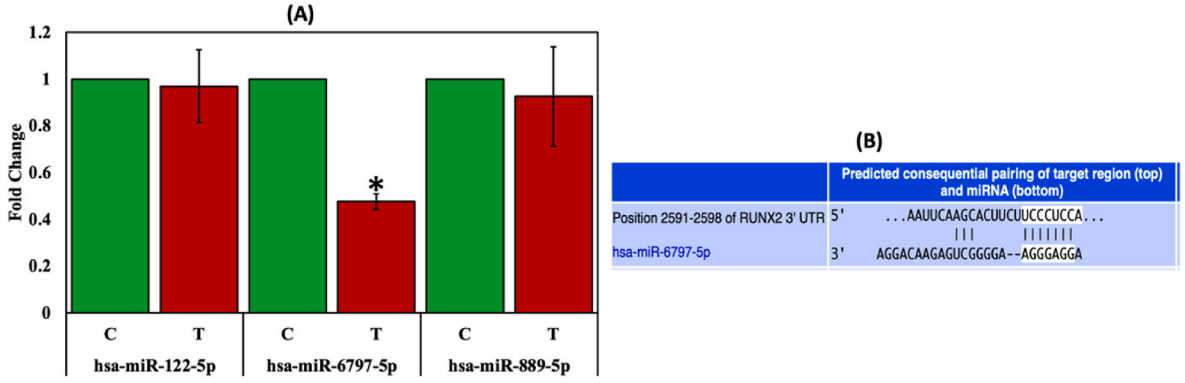

Fig. 4. (A) Expression of selected Runx2-targeting miRNAs in MSCs treated with ovine bone graft-conditioned medium. (B) Predicted binding interaction between hsa-miR-6797-5p and the 3′ untranslated region (3′UTR) of human RUNX2 mRNA. The diagram illustrates the consequential base pairing between hsa-miR-6797-5p and its predicted target site within position 2591–2598 of the RUNX2 3′UTR, as identified by in silico analysis (Target scan). The interaction displays a perfect 8mer seed match, indicating a strong and specific miRNA-mRNA binding potential. This suggests that hsa-miR-6797-5p may directly regulate RUNX2 expression post-transcriptionally, contributing to the modulation of osteogenic signalling pathways.

regulator of RUNX2, and that its suppression by OBG-CM could relieve inhibitory pressure on RUNX2 expression. This provides a mechanistic link between ovine xenograft exposure and modulation of osteogenic signaling pathways, supporting a model in which graft-derived cues influence lineage commitment through selective remodeling of the miRNA landscape.

3.5. Functional validation of hsa-miR-6797-5p in regulating RUNX2 expression

Although multiple RUNX2-targeting miRNAs exhibited down-regulation following OBG-CM exposure, hsa-miR-6797-5p was prioritized for functional validation based on several criteria. First, TargetScan analysis identified a conserved 8-mer seed match within the RUNX2 3′UTR, indicating a high-confidence and potentially dominant regulatory interaction. Second, miR-6797-5p demonstrated the most consistent and pronounced suppression across both osteoblastic cells and MSCs. Third, unlike miR-122-5p and miR-889-5p—which are broadly implicated in metabolic or stress-response pathways—miR-6797-5p has limited prior characterization in bone biology, enhancing the novelty of its investigation. Finally, previous reports linking miR-6797-5p to hormonal regulation of RUNX2 provided a biologically plausible framework for its involvement in graft-mediated osteogenic priming.

To directly test whether hsa-miR-6797-5p regulates RUNX2, osteoblastic cells were transfected with either a synthetic mimic, an inhibitor, or a non-targeting control miRNA. RUNX2 mRNA levels were quantified by qRT-PCR 24 h post-transfection, and protein levels were assessed by Western blotting. As shown in Fig. 5 (left panel), inhibition of hsa-miR-6797-5p resulted in a significant upregulation of RUNX2 transcript levels compared with the control group, whereas transfection with the mimic caused a marked reduction in RUNX2 expression. These opposing effects confirm a negative regulatory role for hsa-miR-6797-5p on RUNX2 transcription. Consistent with the transcript data, Western blot analysis (Fig. 5, right panel) demonstrated elevated RUNX2 protein levels in inhibitor-treated cells and decreased expression in mimic-treated cells relative to controls, with β-actin serving as the internal reference. Together, these results establish hsa-miR-6797-5p as a functional post-transcriptional repressor of RUNX2. The data further suggest that the downregulation of hsa-miR-6797-5p observed in response to ovine bone graft–conditioned medium may relieve inhibitory pressure on RUNX2, thereby promoting osteogenic gene expression.

3.6. Transcription factor regulatory networks associated with RUNX2-targeting miRNAs

To extend the functional interpretation of RUNX2-targeting miRNAs, transcription factor (TF) regulatory networks were constructed using the RegNetwork platform, as described in the Materials and Methods. This approach allowed visualization of how individual miRNAs may

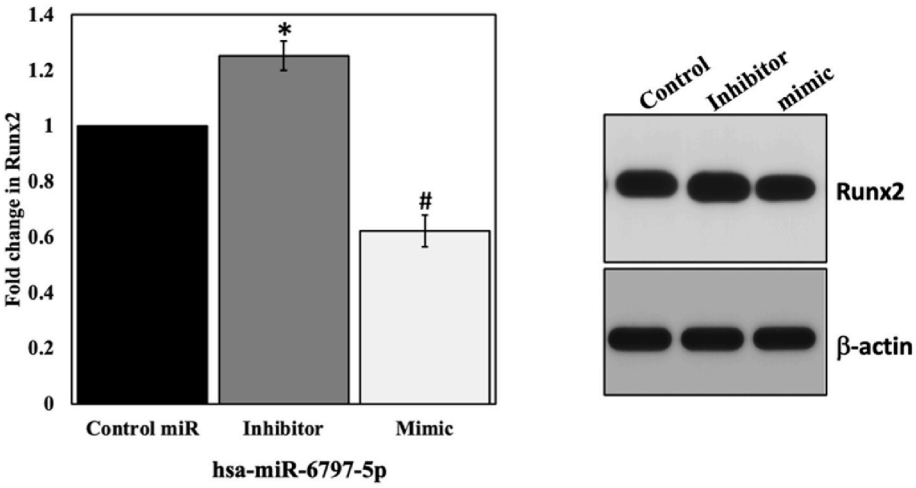

Fig. 5. Effect of hsa-miR-6797-5p mimic and inhibitor on RUNX2 expression in human osteoblastic cells. Left: Bar graph showing fold change in RUNX2 mRNA expression (mean ± SD) in human osteoblastic cells transfected with miR-6797-5p mimic, inhibitor, or control miRNA, assessed by real-time RT-PCR after 24 h. Transfection with the mimic significantly reduced RUNX2 expression, while the inhibitor upregulated RUNX2, indicating a negative regulatory role of miR-6797-5p on RUNX2 transcription. Right: Representative Western blot images showing RUNX2 protein levels (top panel) and β-actin as the loading control (bottom panel) in the same treatment groups. Consistent with mRNA findings, RUNX2 protein levels were suppressed in mimic-treated cells and elevated in inhibitor-treated cells compared to the control group. These data support the post-transcriptional regulatory role of miR-6797-5p in osteogenic gene expression.

integrate into broader transcriptional circuits by regulating or being regulated by key TFs involved in osteogenesis. As illustrated in Fig. 6, three representative networks are displayed. The left panel shows the regulatory interactions of hsa-miR-122-5p, which was predicted to interface with multiple osteogenic regulators including SP1, NF-κB, HIF1A, FOXA1/2, and STAT2. The central panel depicts the expanded network for a broader set of RUNX2-targeting miRNAs, revealing extensive connectivity to transcriptional regulators across diverse pathways, highlighting the potential for combinatorial regulation. The right panel focuses on hsa-miR-889, which demonstrated direct links to TFs such as SMAD4, TEAD family members, and FOXO1, all of which have established roles in osteoblast lineage specification and matrix gene regulation. These network maps reinforce the concept that RUNX2-targeting miRNAs do not act in isolation but are embedded within multi-layered transcriptional circuits, interfacing with master regulators of osteogenesis and stress-responsive pathways. The identification of nodes such as NF-κB, SMADs, and FOX proteins suggests potential convergence points where ovine bone graft–induced miRNA changes could influence osteogenic fate decisions through cross-talk with TF-driven signalling.

4. Discussion

Bone regeneration depends on the coordinated regulation of transcriptional programs, signalling cascades, and epigenetic modulators, with RUNX2 positioned as the pivotal transcription factor driving osteoblast lineage commitment. Hormonal regulation plays a pivotal role in craniofacial bone remodeling, as systemic hormones such as estrogen, parathyroid hormone, vitamin D, and growth hormone modulate osteoblast–osteoclast coupling, thereby influencing bone turnover, mineral density, and adaptive responses unique to the craniofacial skeleton compared with axial and appendicular bones.[24] In the present study, we examined how soluble factors released from ovine bone grafts influence the microRNA (miRNA) network surrounding RUNX2. By integrating in silico predictions with expression analysis and functional assays, we identified hsa-miR-6797-5p as a key post-transcriptional regulator of RUNX2, whose suppression in response to ovine bone graft–conditioned medium (OBG-CM) relieves inhibition of RUNX2 expression. These findings provide mechanistic insight into how xenograft-derived cues may promote osteogenesis by modulating miRNA expression.

The role of miRNAs in osteogenic regulation has been extensively documented. Multiple studies have shown that specific miRNAs directly target RUNX2 and negatively regulate osteoblast differentiation. For example, miR-30a-5p suppresses RUNX2 expression in MC3T3-E1 pre-osteoblasts, attenuating osteogenic differentiation particularly under inflammatory conditions.[23] Similarly, miR-468-3p was reported to inhibit osteogenesis in bone marrow stromal cells by directly binding to RUNX2, with inhibition of this miRNA enhancing osteogenic marker

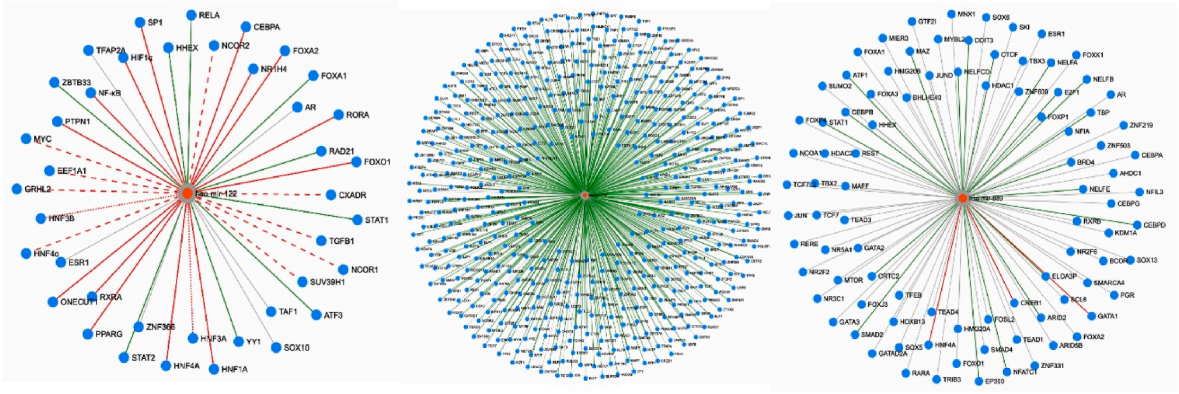

Fig. 6. Transcription factor (TF) regulatory networks of miRNAs targeting RUNX2 constructed using Reg Network.

expression and bone formation in vivo.[25] These observations reinforce the centrality of RUNX2-targeting miRNAs as molecular switches that balance lineage progression.

Among the lesser-studied regulators, miR-6797-5p has recently emerged as an important modulator of RUNX2. Arumugam et al. (2019) demonstrated that parathyroid hormone (PTH) stimulation of osteoblast differentiation increases miR-6797-5p, which in turn represses RUNX2 through direct binding to its 3′UTR. They further showed that a long non-coding RNA (RUNX2-AS1:32) functions as a sponge to sequester miR-6797-5p, thereby protecting RUNX2 expression.[26] Our findings align with this earlier report, as we observed that transfection with a miR-6797-5p mimic reduced RUNX2 expression at both mRNA and protein levels, while inhibitor treatment led to its upregulation. Importantly, OBG-CM exposure selectively suppressed endogenous miR-6797-5p expression, consistent with the idea that xenograft-derived soluble factors can shift the balance of miRNA-mediated repression to favour RUNX2 expression.

Beyond RUNX2, xenograft modulation of other miRNAs has been reported. CCN3, a matricellular protein, was shown to increase RUNX2 and Osterix expression by suppressing miR-608 in osteoblasts through PI3K/Akt signalling.[27] This highlights a broader principle whereby external signals—including proteins, ions, or graft-derived molecules—fine-tune miRNA levels and, in turn, transcriptional outputs. In our study, the selective downregulation of miR-6797-5p, miR-889-5p, and miR-122-5p by OBG-CM suggests that ovine grafts do not globally alter miRNA profiles but instead target specific inhibitory regulators, thereby creating a permissive environment for osteogenic gene expression.

The transcription factor network analysis further supported this interpretation. miRNAs targeting RUNX2, such as miR-122-5p and miR-889, were found to be embedded within regulatory circuits involving NF-κB, SMADs, FOX proteins, and STATs. These nodes are central to osteogenesis and inflammation, suggesting that graft-induced modulation of miRNAs may influence not only RUNX2 expression directly but also the broader transcriptional crosstalk that governs osteoblast differentiation. Similar integrative models have been proposed in recent reviews emphasizing the complex interplay between miRNAs and canonical pathways such as BMP/TGF-β and Wnt signalling.[28]

Taken together, our findings suggest a mechanism in which ovine bone grafts release soluble cues capable of downregulating inhibitory miRNAs like miR-6797-5p, thereby lifting repression on RUNX2. This, in turn, may activate downstream osteogenic genes such as ALPL, COL1A1, and BGLAP, promoting differentiation and matrix mineralization. While the present data support this hypothesis, further work is necessary to identify the specific molecular components of OBG-CM responsible for miRNA modulation. Proteomic and metabolomic analyses may help characterize these factors, while luciferase reporter assays could provide direct confirmation of RUNX2 3′UTR targeting in osteoblastic cells. There are limitations that should be acknowledged. The study focused on short-term (24 h) exposure to OBG-CM; longer incubation times may reveal additional dynamics in miRNA regulation and RUNX2 expression. Moreover, in vitro experiments in isolated osteoblasts or MSCs cannot fully capture the complexity of bone healing, which involves osteoclasts, immune cells, and angiogenic support. In vivo validation using xenograft implantation models would therefore be an important next step. Despite these limitations, the present findings highlight an underexplored dimension of graft biology—the capacity to modulate post-transcriptional regulatory circuits that control osteogenic differentiation. This work demonstrates that ovine bone graft–derived factors can selectively alter the expression of RUNX2-targeting miRNAs, with hsa-miR-6797-5p emerging as a key repressor whose downregulation promotes RUNX2 expression. By linking graft-induced molecular changes to a central transcriptional regulator of osteogenesis, these findings provide a mechanistic framework that may guide the rational design and optimization of xenografts and biomaterials for bone regeneration.

5. Limitations and future scope

This work is based on short-term exposure (24 h) to OBG-CM, so later-stage osteogenic outcomes were not directly captured. Also, while TargetScan and the mimic/inhibitor experiments support a RUNX2–miR-6797-5p relationship, a 3′UTR luciferase reporter assay would provide a cleaner, site-specific confirmation of direct binding. Another limitation is that the specific soluble mediators responsible for miRNA suppression were not identified. Future work should fractionate OBG-CM (size/charge-based separation) and apply proteomics/metabolomics or ion profiling to pinpoint candidate drivers. Finally, these findings should be tested in more physiological settings (co-culture with immune/osteoclast lineage cells, and in vivo xenograft implantation models), since inflammation, vascular inputs, and mechanical loading can reshape RUNX2 and miRNA regulation during actual healing. Future studies should extend these observations in vivo and identify the specific molecular components within graft-conditioned media that are responsible for these effects. In summary, ovine-derived grafts appear to enhance osteogenic commitment through selective remodeling of miRNA networks, offering new opportunities for biomaterial optimization in regenerative dentistry and orthopaedics.

6. Conclusion

The findings of this study indicate that ovine bone graft–conditioned medium selectively modulates RUNX2-targeting microRNAs during early exposure, with hsa-miR-6797-5p emerging as a functionally relevant post-transcriptional regulator. While these results do not directly demonstrate osteogenic differentiation, they identify a plausible early molecular mechanism through which ovine grafts may prime osteoblast-lineage cells by relieving inhibitory control over RUNX2.

Ethical clearance

Not applicable.

Patient's/Guardian's consent

Not applicable.

Source of funding

Nil.

Declaration of competing interest

The authors declare that they have no known competing financial interests or personal relationships that could have appeared to influence the work reported in this paper.

Acknowledgment

Nil.

References

1. Nishal S, Phaugat P, Devi R, et al. Harnessing 3D printing in bone tissue engineering. *Discov Mater*. 2025;5(1):135.
2. Dam VV, Trinh HA, Rokaya D, Trinh DH. Bone augmentation for implant placement: recent advances. *Int J Dentistry*. 2022;2022(1), 8900940.
3. Bucchi C, Del Fabbro M, Arias A, et al. Multicenter study of patients' preferences and concerns regarding the origin of bone grafts utilized in dentistry. *Patient Prefer Adherence*. 2019;13:179–185.
4. Inose H, Ochi H, Kimura A, et al. A microRNA regulatory mechanism of osteoblast differentiation. *Proc Natl Acad Sci USA*. 2009;106(49):20794–20799.
5. Vohra M, Maiti S, Shah KK, et al. Influence of L-arginine on hydroxyapatite-based ovine bone graft - an in vitro evaluation of surface characteristics and cell viability. *Dent Res J*. 2025;22(5):19.

6. Khurshid Z, Alfarhan MF, Mazher J, et al. Extraction of hydroxyapatite from camel bone for bone tissue engineering application. *Molecules*. 2022 Nov 16;27(22):7946.
7. Khurshid Z, Alfarhan MF, Bayan Y, et al. Development, physicochemical characterization and in-vitro biocompatibility study of dromedary camel dentine derived hydroxyapatite for bone repair. *PeerJ*. 2023 Aug 3;11, e15711.
8. Khurshid Z, Adanir N, Ratnayake J, Dias G, Cooper PR. Demineralized dentin matrix for bone regeneration in dentistry: a critical update. *Saudi Dental J*. 2024 Mar 1;36 (3):443–450.
9. Banstola A, Reynolds JNJ. The sheep as a large animal model for the investigation and treatment of human disorders. *Biology*. 2022;11(9):1251.
10. Scarano A, Khater AGA, Gehrke SA, et al. Animal models for investigating osseointegration: an overview of implant research over the last three decades. *J Funct Biomater*. 2024;15(4).
11. Zhu S, Chen W, Masson A, et al. Cell signaling and transcriptional regulation of osteoblast lineage commitment, differentiation, bone formation, and homeostasis. *Cell Disc*. 2024;10(1):1–39.
12. Kanatani N, Fujita T, Fukuyama R, et al. Cbfβ regulates Runx2 function isoform-dependently in postnatal bone development. *Dev Biol*. 2006 Aug 1;296(1):48–61.
13. Hojo H, Saito T, He X, et al. Runx2 regulates chromatin accessibility to direct the osteoblast program at neonatal stages. *Cell Rep*. 2022;40(10), 111315.
14. Kp A, Kaliaperumal K, Sekar D. microRNAs and their therapeutic strategy in phase I and phase II clinical trials. *Epigenomics*. 2024;16(4):259–271.
15. Selvakumar SC, Preethi KA, Ross K, Sekar D. The emerging role of microRNA-based therapeutics in the treatment of preeclampsia. *Placenta*. 2024;158:38–47.
16. Ameya KP, Usman PAS, Sekar D. Navigating the tumor landscape: VEGF, MicroRNAs, and the future of cancer treatment. *Biochim et Biophys Acta Gene Regul Mech*. 2025, 195091.
17. Huang J, Zhao L, Xing L, et al. MicroRNA-204 regulates Runx2 protein expression and mesenchymal progenitor cell differentiation. *Stem Cell*. 2010;28(2):357–364.
18. Wu T, Zhou H, Hong Y, et al. miR-30 family members negatively regulate osteoblast differentiation. *J Biol Chem*. 2012;287(10):7503–7511.
19. Limlawan P, Marger L, Durual S, et al. Delivery of microRNA-302a-3p by APTES modified hydroxyapatite nanoparticles to promote osteogenic differentiation in vitro. *BDJ Open*. 2023;9(1):8.
20. Development of miR-26a-activated scaffold to promote healing of critical-sized bone defects through angiogenic and osteogenic mechanisms. *Biomaterials*. 2023;303, 122398.
21. Jiménez-Ortega RF, Ortega-Meléndez AI, Patiño N, et al. The involvement of microRNAs in bone remodeling signaling pathways and their role in the development of osteoporosis. *Biology (Basel) [Internet]*. 2024;13(7).
22. Wu F, Song C, Zhen G, et al. Exosomes derived from BMSCs in osteogenic differentiation promote type H blood vessel angiogenesis through miR-150-5p mediated metabolic reprogramming of endothelial cells. *Cell Mol Life Sci*. 2024;81 (1):344.
23. Liu X, Liu H, Chen J, Yang X, He Q, Chen L. miR-30a-5p inhibitors promote osteogenesis by targeting Runx2 in MC3T3-E1 under inflammation. *BMC Oral Health*. 2021;21(1):331.
24. Tunheim EG, Skallevold HE, Rokaya D. Role of hormones in bone remodeling in the craniofacial complex: a review. *J Oral Biol Craniofacial Res*. 2023 Mar 1;13(2): 210–217.
25. Fang T, Zhang R, Song F, et al. miR-468-3p suppresses osteogenic differentiation of BMSCs by targeting Runx2 and inhibits bone formation. *J Orthop Surg Res*. 2024;19: 887.
26. Arumugam B, Mohanakrishnan V, Shreya S, Selvamurugan N. Parathyroid hormone stimulation of Runx2 during osteoblast differentiation via the regulation of lnc-SUPT3H-1:16 (RUNX2-AS1:32) and miR-6797-5p. *Biochimie*. 2019;158:43–52.
27. Chen P-C, Liu J-F, Fong Y-C, Huang Y-L, Chao C-C, Tang C-H. CCN3 facilitates Runx2 and osterix expression by inhibiting miR-608 through PI3K/Akt signaling in osteoblasts. *Int J Mol Sci*. 2019;20(13):3300.
28. Loh H-Y, Norman BP, Lai K-S, et al. Post-transcriptional regulatory crosstalk between MicroRNAs and canonical TGF-β/BMP signalling cascades on osteoblast lineage: a comprehensive review. *Int J Mol Sci*. 2023;24(7):6423.